

research article

Portal hypertension may influence the registration of hypointensity of small hepatocellular carcinoma in the hepatobiliary phase in gadoxetic acid MR

Carla Caparroz¹, Alejandro Forner^{2,3}, Jordi Rimola, Anna Darnell¹, Ángeles García-Criado¹, Juan Ramón Ayuso¹, María Reig^{2,3}, Jordi Bruix^{2,3}, Carmen Ayuso^{1,3}

¹ Radiology Department, Barcelona Clinic Liver Cancer (BCLC) Group, Hospital Clinic Barcelona, University of Barcelona, Spain

² Liver Unit, Barcelona Clinic Liver Cancer (BCLC) Group, Hospital Clinic Barcelona. IDIBAPS, University of Barcelona, Spain

³ Centro de Investigación Biomédica en Red de Enfermedades Hepáticas y Digestivas (CIBERehd), Barcelona, Spain

Radiol Oncol 2022; 56(3): 292-302.

Received 4 February 2022

Accepted 24 April 2022

Correspondence to: Prof. Carmen Ayuso, M.D., Radiology Department. BCLC group. Hospital Clínic, c/ Villarroel, 170. Escala 3, Planta 1. 08036. Barcelona. Spain. E-mail: cayuso@clinic.cat

Disclosure: Carla Caparroz and Juan Ramón Ayuso report no conflict of interest; Alejandro Forner: Lecture fees from Bayer, Gilead, Boston Science and MSD. Consultancy fees from Bayer, AstraZeneca, Roche, SIRTEX, AB Exact Science and Guerbert; Anna Darnell: speaker fees and travel grants from Bayer; Jordi Rimola: speaker fees and travel grants from Bayer and BTG and Terumo, consultancy fees from Roche and COR2ED; Ángeles García-Criado: speaker fees from BTG and Terumo; María Reig: Lecture fees from Gilead, BMS, BTG, Eisai, Lilly, and Bayer. Consultancy fees from Bayer, BMS, AstraZeneca, ROCHE, Lilly, Ipsen and Boston Scientific. Research grants from Bayer and Ipsen; Jordi Bruix: Consultancy fees from Arqule, Bayer-Shering Pharma, Novartis, BMS, BTG-Biocompatibles, Eisai, Kowa, Terumo, Gilead, Bio-Alliance, Roche, AbbVie, MSD, Sirtex, Ipsen, Astra-Medimmune, Incyte, Quirem, Adaptimmune, Lilly, Basilea, Nerviano, Sanofi. Research grants from Bayer. Educational grants from Bayer. Lecture fees from Bayer, BTG, AstraZeneca Eisai, Terumo, Sirtex, and Ipsen.

Carla Caparroz and Alejandro Forner contributed equally and share the first authorship.

This is an open access article under the CC BY-NC-ND license (<http://creativecommons.org/licenses/by-nc-nd/4.0/>).

Background. The aim of the study was to analyze the association between the liver uptake of Gadolinium-ethoxybenzyl-diethylenetriamine penta-acetic acid (Gd-EOB-DTPA) in the hepatobiliary phase (HBP) in cirrhotic patients and the presence of clinically significant portal hypertension (CSPH), and how these features impact on hepatocellular carcinoma (HCC) detection in the HBP.

Patients and methods. Post-hoc analysis of a prospective cohort of 62 cirrhotic patients with newly US-detected nodule between 1–2 cm (study group). Twenty healthy subjects were used as control group. Qualitative and quantitative analysis of the liver contrast uptake in the HBP assessed by Relative Liver-Enhancement (RLE), Liver-Spleen (LSCR), Liver-Muscle (LMCR), and Liver-Kidney Contrast-Ratio (LKCR), Contrast Enhancement Index (CEI), and Hepatic Uptake (HUI), and biliary excretion, were registered. CSPH was confirmed invasively (HVPG > 10 mmHg) or by indirect parameters. The appearance of HCC at the HBP was analyzed.

Results. Nineteen patients (30.6%) did not have CSPH. In 41 patients (66.1%) the final diagnosis was HCC. All indices were significantly higher in the control group, indicating a more intense HBP liver signal intensity compared to patients with cirrhosis, even if the comparison was restricted to patients with no CSPH. CSPH was associated to a lower rate of HCC hypointensity in the HBP (51.9% vs. 85.7% without CSPH, $p = 0.004$).

Conclusions. Liver uptake of Gd-EOB-DTPA at the HBP is decreased in cirrhosis even if the liver function is minimally impaired and it falls down significantly in patients with CSPH compromising the recognition of hypointense lesions. This fact may represent a limitation for the detection of small HCC in patients with cirrhosis and CSPH.

Key words: liver cirrhosis; magnetic resonance imaging; hepatocellular carcinoma

Introduction

Portal hypertension (PH) is a clinical syndrome that often complicates cirrhosis. It is related to the increased hepatic resistance to portal blood flow through the liver because of the architectural disruption of the liver vascular anatomy caused by fibrosis and nodule formation.¹ An important step in the pathophysiology of PH is the dysfunction at the hepatic sinusoidal cells in response to different liver injuries in the early stages of the cirrhosis development.¹ PH is defined as clinically significant (CSPH) when the portal pressure increases above a critical threshold value of 10 mmHg.² Although under this value there are no complications related to PH (such as ascites or variceal bleeding), significant changes in the hepatic sinusoidal system are already present in cirrhotic patients with hepatic venous pressure gradient below 10 mmHg. Interestingly, development of CSPH is the well-established key event defining a clinically significant risk of hepatocellular carcinoma development.³⁻⁵

Gadolinium-ethoxybenzyl-diethylenetriamine penta-acetic acid (Gd-EOB-DTPA; Primovist/Eovist®), also known as gadoxetic acid, has an early phase with distribution into the extracellular space similar to other gadolinium-based contrast agents, followed by the uptake into hepatocytes and excretion into bile during the hepatobiliary phase (HPB).⁶⁻⁸ The uptake of Gd-EOB-DTPA by the hepatocytes during this delayed phase is impaired in chronic liver diseases and in recent years, there have been several attempts to evaluate the potential of magnetic resonance (MR) with Gd-EOB-DTPA as a reliable tool for liver dysfunction assessment.⁹ Increased model for end-stage liver disease (MELD), bilirubin and indocyanine green clearance ratio at 15 minutes, and decreased cholesterol have been associated with suboptimal HBP¹⁰⁻¹⁴, and the parenchymal enhancement among different HBP phases (at 5, 10, 15 and 20 minutes) is lower in Child-Pugh (CP) B and C compared to CP-A patients.^{15,16} Also, MR with Gd-EOB-DTPA has been tested for preoperative identification of those patients with major contraindications for hepatectomy.¹⁷⁻²⁰

A recent experimental study in animals evaluating the impact of PH in the pharmacokinetics of gadobenate dimeglumine (Gd-BOPTA) has shown that the clearance across sinusoidal membranes of contrast agents is modified by changes in portal flow rates and as a result, at a given perfused concentration, portal flow rates modified Gd-BOPTA hepatocyte concentrations.²¹ However, the impact

of these changes related to PH in the contrast uptake in the HBP and in the diagnostic accuracy of the MR with Gd-EOB-DTPA has not been extensively studied.

Accordingly, the aim of the present study is to evaluate the impact of CSPH and liver function impairment on the liver uptake of Gd-EOB-DTPA during the HBP, and consequently, how they may impact on hepatocellular carcinoma (HCC) detection in the HBP.

Patients and methods

Between July 2012 and October 2015, we prospectively included consecutive asymptomatic patients with Child-Pugh A-B cirrhosis with no previous history of hepatocellular carcinoma (HCC), in whom a new solitary well defined solid nodule between 1 and 2 cm was detected by screening ultrasonography (US). The Institutional Ethics Committee for Clinical Research approved the study and all patients provided written informed consent before enrollment. These patients were included in a prospective study conducted in our Unit.²² Hepatic extracellular-contrast-enhanced MR (EC-MR) followed by Gd-EOB-DTPA MR were obtained in less than 1-month interval. The final HCC diagnosis was established by EC-MR according to the accepted non-invasive criteria⁵, or by biopsy in lesions with atypical vascular profile. All these patients (n = 62) were considered the study group. We also included patients with healthy liver who were submitted to Gd-EOB-DTPA MR for the study of a solitary hepatocellular liver lesion (focal nodular hyperplasia, or hepatocellular adenoma) during the same period, and they were included as a control group for evaluating the liver uptake of Gd-EOB-DTPA during HBP (control group).

Diagnosis of CSPH in patients in the study group was established based on Baveno recommendations² including 1) hepatic venous pressure gradient (HVPG) greater than 10 mm Hg, or 2) by indirect clinical findings when: a) the hepatic elastography (Fibroscan®-Echosens, Paris, France) registered a value greater than 21 Kpa,²³ b) presence of venous shunts, and/or ascites at imaging techniques and/or 3) presence of gastroesophageal varices by upper endoscopy.

MR imaging

Two 1.5-T MR units were used: SIGNA HDxt, GE Healthcare and Magnetom AERA, Siemens

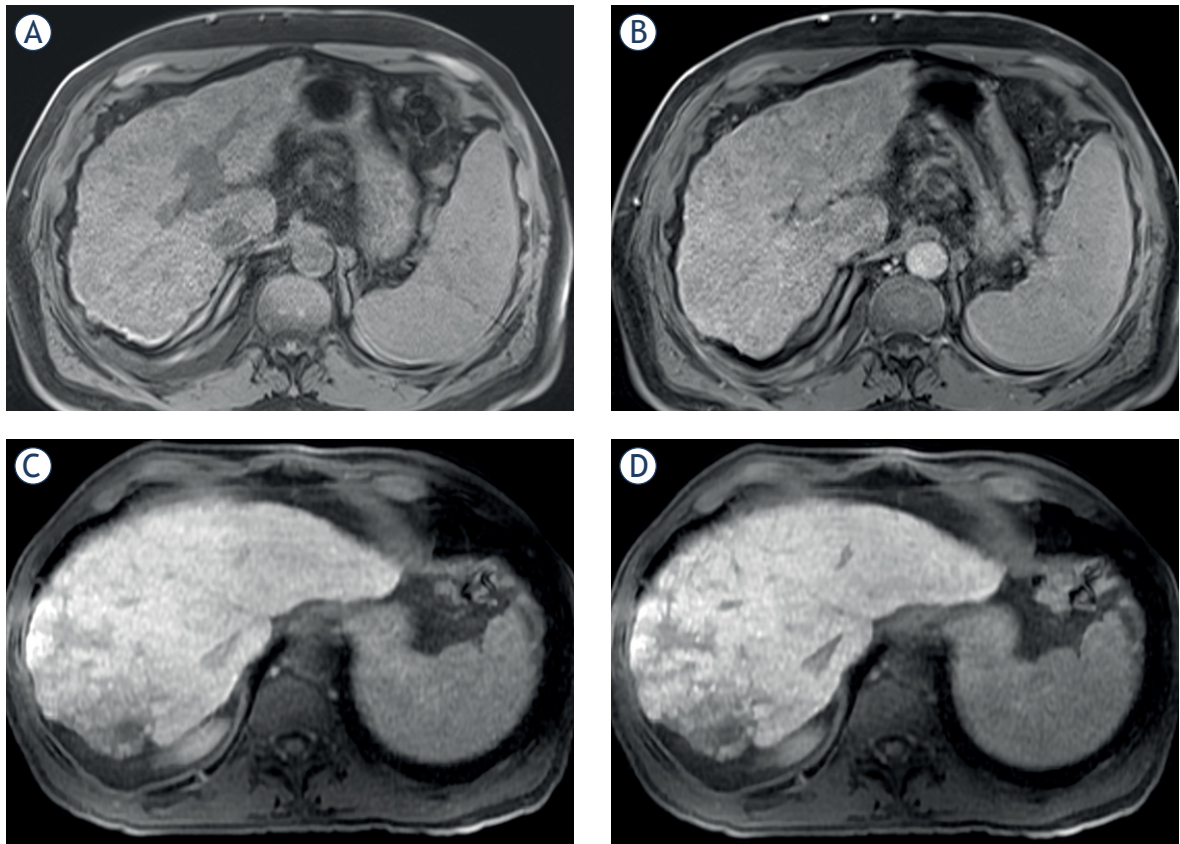


FIGURE 1. Non-adequate quality in the liver uptake of Gadolinium-ethoxybenzyl-diethylenetriamine penta-acetic acid (Gd-EOB-DTPA) in the 20 minutes hepatobiliary phase. **(A)** and **(B)**: patient with liver cirrhosis Child-Pugh B and clinically significant portal hypertension. **(A)**: Baseline T1w-3D VIBE sequence. **(B)**: the liver showed poor or non-apparent contrast uptake compared to the liver before contrast injection. **(C)** and **(D)**: patient with liver cirrhosis Child-Pugh A 5 points with no clinically significant portal hypertension. **(C)**: Baseline T1w-3D VIBE sequence. **(D)**: the liver parenchyma showed very heterogeneous uptake of the contrast media, especially in the periphery of the right hepatic lobe.

Medical Solutions. The sequence protocol for Gd-EOB-DTPA MR is detailed in supplemental material. Dynamic images were acquired after IV injection of gadoxetic acid 0,25 mmol/ml (Primovist; Bayer) at a dose of 0.1 ml/kg body weight at a rate of 1,5 ml/s followed by a 20 ml saline flush at the same rate. The arterial phase was acquired 7 s after the arrival of contrast medium in the aortic arch. Portal and transitional and HB phases were acquired 50 s, 90 s, 10 min and 20 min thereafter respectively. The 20 minutes HBP was not acquired in those patients without underlying chronic liver disease.

Evaluation of liver uptake of Gd-EOB-DTPA in the hepatobiliary phase

Qualitative analysis

All 10 and 20 minutes HBPs were reviewed by two independent radiologists (A.D. and J.R.). The qual-

ity of the HBP was classified as 1) adequate, when the liver parenchyma showed signal intensity (SI), higher than the SI of the intrahepatic vessels, or 2) Non-adequate quality, when the SI in the liver parenchyma was non-superior to the SI in intrahepatic vessels (Figure 1).²⁴ Also, the biliary contrast excretion was evaluated qualitatively according to the extension (intrahepatic only and extrahepatic). Inadequate hepatobiliary contrast excretion was defined as the lack of contrast agent in the extrahepatic bile ducts in the hepatobiliary phase at 20 minutes

Quantitative analysis

Different MR-derived parameters focused to estimate the amount of Gd-EOB-DTPA liver uptake were calculated in the 10 and 20 minutes HBP. In all these indices, greater values mean more liver uptake of Gd-EOB-DTPA in the HBP. The quantita-

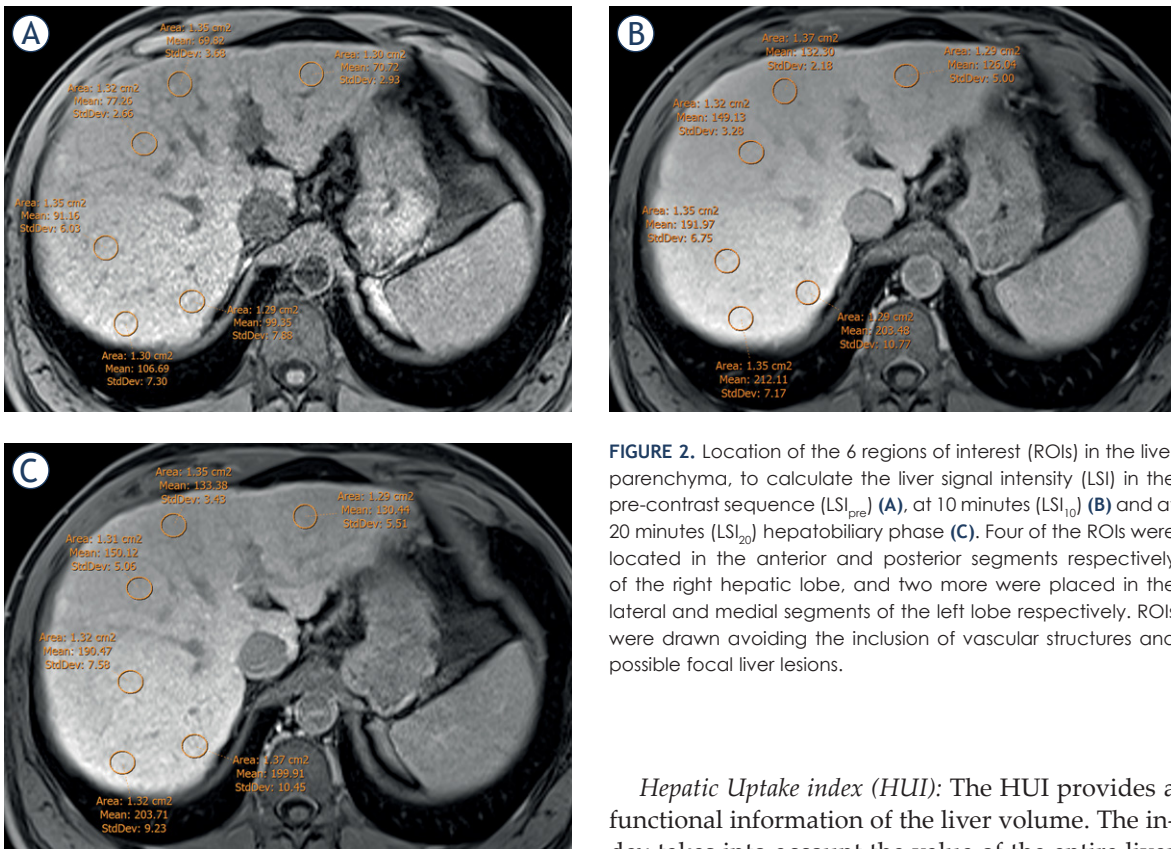


FIGURE 2. Location of the 6 regions of interest (ROIs) in the liver parenchyma, to calculate the liver signal intensity (LSI) in the pre-contrast sequence (LSI_{pre}) (A), at 10 minutes (LSI₁₀) (B) and at 20 minutes (LSI₂₀) hepatobiliary phase (C). Four of the ROIs were located in the anterior and posterior segments respectively of the right hepatic lobe, and two more were placed in the lateral and medial segments of the left lobe respectively. ROIs were drawn avoiding the inclusion of vascular structures and possible focal liver lesions.

tive assessments were done by C.C. (Figure 2). All formulas are summarized in Table 1 and described in detail in supplemental material.

Relative Liver Enhancement (RLE): RLE₁₀ and RLE₂₀ establish the relationship between the SI of the liver parenchyma in the 10 minutes (LSI₁₀) and the 20 minutes HBP (LSI₂₀), and the liver SI before contrast injection (LSI_{pre}).²⁵

Liver to Spleen/muscle/Kidney Contrast Ratios: These indices determine the relationship between the SI of the liver and the SI of the spleen (LSCR), muscle (LMCR) and kidney (LKCR). To estimate the LSCR, an additional ROI was drawn on the spleen, over the same three images selected previously.²⁶ (Figure 3A) For LMCR, an additional ROI with an average area of 100 mm² was drawn on the right paraspinal muscle. (Figure 3B). Finally, for LKCR an additional ROI with an average area of 0,5 to 1 cm² was drawn on the upper pole of the right kidney (Figure 3C).

Contrast Enhancement Index (CEI): The CEI₁₀ and CEI₂₀ were calculated as a ratio between the liver-to-muscle SI ratio 10 and 20 minutes after contrast injection (LMCR₁₀ and LMCR₂₀) respectively, and the liver-to muscle SI ratio before contrast injection (LMCR_{pre}).²⁷

Hepatic Uptake index (HUI): The HUI provides a functional information of the liver volume. The index takes into account the value of the entire liver volume (Vol_{Liver}), and the liver and spleen signal intensity and the formula is described in Table 1. Vol_{Liver} was calculated in the late venous T1WI sequence obtained 5 minutes after contrast injection. For this purpose, a free hand irregular-ROI was drawn delineating the liver contour in every one of the images (ALMA 3D Workstation®), defining a liver area by liver plane. The Vol_{Liver} expressed in cm³ was the sum of all the measured liver areas.

Analysis of the focal liver lesions

The imaging characteristics of the target lesion (TL) were independently registered in an electronic case report form by A.D. and J.R. They were blinded to final diagnosis, and imaging findings registered by each other. Any discrepancies during image analysis were solved by consensus discussion between the two investigators. Qualitative appearance of the lesion on delayed post-contrast sequences were registered as hypo, hyper or isointense lesions respect to the surrounding liver parenchyma.

Statistical analysis

Baseline characteristics of the patients were expressed as median and range or count and propor-

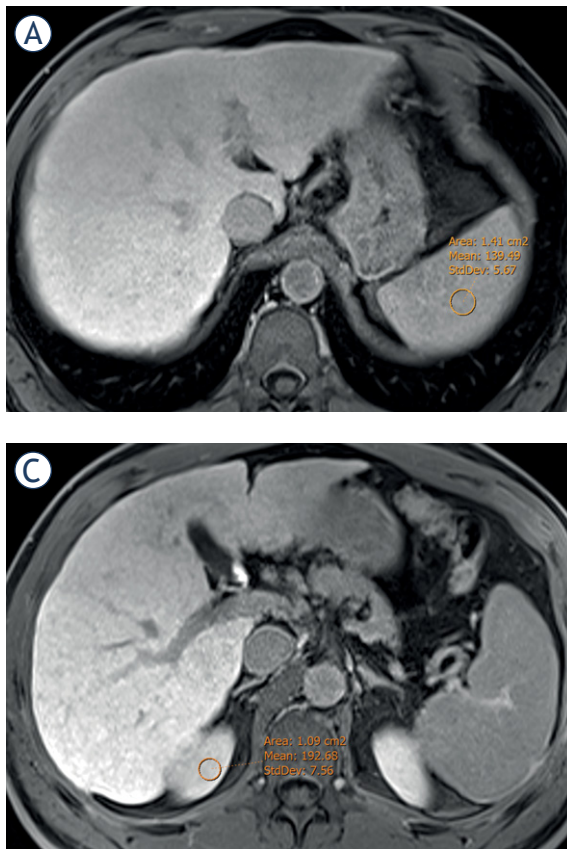


FIGURE 3. Location of the region of interest in the 20 minutes hepatobiliary phase in the spleen (A), in the right paravertebral muscle (B), and in the upper pole of the right kidney (C) to calculate the different quantitative parameters of contrast liver uptake: spleen-liver intensity (SLI) and liver-spleen contrast ratio (LSCR), muscle-liver intensity (MLI) and the liver-muscle contrast ratio (LMCR) and kidney-liver intensity (KLI) and the liver-kidney contrast ratio (LKCR), respectively.

tion. Comparisons were done by using the Student *t* test or the Mann-Whitney test for continuous variables and the chi-square test or Fisher-exact test for categorical variables. A *p* value of less than 0.05 was considered significant. Calculations were done with the SPSS package version 20 (SPSS, Inc., Chicago, IL)

Results

A total of 62 cirrhotic patients were included in the study group and their characteristics are summarized in supplemental Table 1. Fifty-three out of 62 (85.5%) were CP-A patients [A-5 points (*n* = 44) and A-6 points (*n* = 9)] and 9 (14.5%) were CP-B [B-7 points (*n* = 4), B-8 points (*n* = 4) and B-9 points (*n* = 1)]. Forty-three (69.4%) had CSPH: 11 confirmed by HVPG > 10 mm Hg (*n* = 11) and 32 by indirect signs. All patients with Child-Pugh score ≥ 6 (*n* = 18) had CSPH. The control group included 20 patients without chronic liver disease and normal liver function.

Final diagnosis of the 62 target lesions in the study group patients was: HCC (*n* = 41; 66.1%), intrahepatic cholangiocarcinoma (ICC) (*n* = 2;

3.2%), colorectal cancer metastases (*n* = 1; 1.6%), and benign conditions (angioma, *n* = 2; Dysplastic/regenerative nodules, *n* = 4 and unspecific benign lesions, *n* = 12).²² The HBP at 20 minutes was not available in one patient with a final diagnosis of HCC. Thirty-one out of 41 HCC were diagnosed by non-invasive criteria (in 8 cases, pathology confirmation was also available) and by pathology in the remaining 10 cases.

Impact of liver function on the Gd-EOB-DTPA uptake in the HBP

Table 2 describes the different quantitative parameters evaluating the contrast liver uptake in the 10 and 20 minutes HBP considering the degree of liver function impairment according to Child-Pugh classification. All quantitative indices were significantly higher in CP-A patients compared to CP-B. We also focused our analysis in those CP-A patients comparing between 5 and 6 points: Except in LMCR, all indices were significantly higher in CP-A 5 points patients.

Impact of CSPH on the Gd-EOB-DTPA liver uptake in the HBP

We further evaluated the impact of CSPH on the liver enhancement in the HBPs (Table 3). All indices except RLE at 20 minutes and CEI were signifi-

TABLE 1. Formulas used for qualitative assessment of liver uptake of Gadolinium-ethoxybenzyl-diethylenetriamine penta-acetic acid (Gd-EOB-DTPA) in the hepatobiliary phase (HPB)

	Formula	Variables definition
Relative Liver Enhancement (RLE)	$RLE_{10} = \frac{(LSI_{10} - LSIPRE)}{LSIPRE}$	RLE ₁₀ and RLE ₂₀ : RLE at 10- and 20-min HPB
	$RLE_{20} = \frac{(LSI_{20} - LSIPRE)}{LSIPRE}$	LSI _{pre} , LSI ₁₀ and LSI ₂₀ : Liver signal intensity pre-contrast, at 10- and 20-min HPB, respectively
Liver to Spleen Contrast Ratio (LSCR)	$LSCR_{pre} = \frac{LSIPRE}{SSIPRE}$	LSCR _{pre} , LSCR ₁₀ and LSCR ₂₀ : LSCR pre-contrast, at 10- and 20- min HPB, respectively
	$LSCR_{10} = \frac{LSI_{10}}{SSI_{10}}$	LSI _{pre} , LSI ₁₀ and LSI ₂₀ : Liver signal intensity pre-contrast, at 10- and 20- min HPB, respectively
	$LSCR_{20} = \frac{LSI_{20}}{SSI_{20}}$	SSI _{pre} , SSI ₁₀ and SSI ₂₀ : Spleen signal intensity pre-contrast, at 10- and 20- min HPB, respectively
Liver to muscle Contrast Ratio (LMCR)	$LMCR_{pre} = \frac{LSIPRE}{MSIPRE}$	LMCR _{pre} , LMCR ₁₀ and LMCR ₂₀ : LMCR pre-contrast, at 10- and 20- min HPB, respectively
	$LMCR_{10} = \frac{LSI_{10}}{MSI_{10}}$	LSI _{pre} , LSI ₁₀ and LSI ₂₀ : Liver signal intensity pre-contrast, at 10- and 20- min HPB, respectively
	$LMCR_{20} = \frac{LSI_{20}}{MSI_{20}}$	MSI _{pre} , MSI ₁₀ and MSI ₂₀ : Muscle signal intensity pre-contrast, at 10- and 20- min HPB, respectively
Liver to Kidney Contrast Ratios (LKCR)	$LKCR_{pre} = \frac{LSIPRE}{KSIPRE}$	LKCR _{pre} , LKCR ₁₀ and LKCR ₂₀ : LKCR pre-contrast, at 10- and 20- min HPB, respectively
	$LKCR_{10} = \frac{LSI_{10}}{KSI_{10}}$	LSI _{pre} , LSI ₁₀ and LSI ₂₀ : Liver signal intensity pre-contrast, at 10- and 20- min HPB, respectively
	$LKCR_{20} = \frac{LSI_{20}}{KSI_{20}}$	KSI _{pre} , KSI ₁₀ and KSI ₂₀ : Kidney signal intensity pre-contrast, at 10- and 20- min HPB, respectively
Contrast Enhancement Index (CEI)	$CEI_{10} = \frac{LMCR_{10}}{LMCR_{pre}}$	- LMCR _{pre} , LMCR ₁₀ and LMCR ₂₀ : LMCR pre-contrast, at 10- and 20- min HPB, respectively
	$CEI_{20} = \frac{LMCR_{20}}{LMCR_{pre}}$	- CEI ₁₀ and CEI ₂₀ : Contrast Enhancement Index at 10- and 20- min HPB, respectively
Hepatic Uptake index (HUI)	$HUI_{10} = VOL_{LIVER} \left(\frac{LSI_{10}}{SSI_{10}} \right) - 1$	- HUI ₁₀ and HUI ₂₀ : Hepatic Uptake index at 10- and 20- min HPB, respectively
	$HUI_{20} = VOL_{LIVER} \left(\frac{LSI_{20}}{SSI_{20}} \right) - 1$	LSI ₁₀ and LSI ₂₀ : Liver signal intensity at 10- and 20- min HPB, respectively SSI ₁₀ and SSI ₂₀ : Spleen signal intensity at 10- and 20- min HPB, respectively

cantly higher in absence of CSPH. To confirm the impact of CSPH irrespectively of liver function, we evaluated those patients with well-preserved liver function (CP-A 5 points) and in them, CSPH impacted in the liver Gd-EOB-DTPA uptake since LSCR, LMCR and LKCR were significantly higher in those patients without CSPH. Finally, we compared the liver contrast uptake in patients with very well-preserved liver function (all CP-A 5 points and those without CSPH) and patients with normal liver (control group B) and all scores were significantly higher in patients with healthy liver (Table 4).

Gd-EOB-DTPA liver uptake through the different HBP (10 and 20 minutes)

The quantitative assessment is exposed in supplemental Table 2. All parameters that quantify the liver contrast uptake were significantly higher at 20 minutes compared to at 10 minutes. These differences were maintained in CP-A and CP-A 5 points patients. The calculations were not done in Child-Pugh B due to low number of patients.

Impact of CSPH over the biliary excretion of Gd-EOB-DTPA in the HBP 20 minutes

In the 49 patients with adequate HBP at 20 minutes, the biliary excretion of the contrast media arrived to the extrahepatic bile duct (n = 20) and the intestinal lumen (n = 28). Contrarily, only in 6 out 12 cases with poor HBP quality, the biliary excretion was present in the extrahepatic bile duct (p < 0.001). In all patients without CSPH (n = 18), the biliary excretion arrived to extrahepatic bile duct. Contrarily, in 7 out of 43 patients with CSPH (16.3%), the biliary excretion was not identified in the extrahepatic biliary tree.

Impact of the quality of the HBP and the presence of CSPH in the registration of hypointense HCC lesions in HBP

In 49 out of 62 MR studies (79%), the HBP was categorized as adequate, in 12 (19.4%) non-adequate and in one patient (1.6%), the 20 minutes HBP was not available. Six out of 12 patients with non-ade-

TABLE 2. Quantitative assessment of liver uptake of Gadolinium-ethoxybenzyl-diethylenetriamine penta-acetic acid (Gd-EOB-DTPA) during the hepatobiliary phase (HPB) at 10 and 20 minutes considering the degree of liver function impairment according to Child-Pugh classification. Variables described as median and interquartile range

INDEX	Study group	Child-Pugh A	Child-Pugh B	P value	Child-Pugh A-5 points	Child-Pugh A-6 points + B	P value
N	62	53	9		44	18	
RLE ₁₀	0.65 [0.49-0.75]	0.68 [0.51-0.81]	0.41 [0.30-0.52]	<0.001	0.68 [0.52-0.82]	0.50 [0.40-0.58]	0.005
RLE ₂₀	0.63 [0.51-0.78]	0.67 [0.55-0.82]	0.41 [0.30-0.52]	<0.001	0.68 [0.56-0.83]	0.52 [0.40-0.61]	0.006
LSCR ₁₀	1.32 [1.17-1.55]	1.35 [1.11-1.59]	1.20 [0.99-1.28]	0.016	1.43 [1.19-1.61]	1.20 [1.11-1.28]	0.001
LSCR ₂₀	1.48 [1.23-1.71]	1.51 [1.30-1.80]	1.20 [1.01-1.43]	0.006	1.54 [1.32-1.81]	1.25 [1.17-1.53]	0.008
LMCR ₁₀	2.14 [1.78-2.51]	2.16 [1.81-2.62]	1.78 [1.52-2.13]	0.030	2.26 [1.81-2.71]	2.08 [1.73-2.16]	NS
LMCR ₂₀	2.25 [1.86-2.63]	2.29 [1.89-2.69]	1.79 [1.52-2.23]	0.030	2.34 [1.88-2.70]	2.05 [1.75-2.31]	NS
LKCR ₁₀	1.02 [0.85-1.17]	1.04 [0.89-1.21]	0.83 [0.74-0.90]	0.005	1.06 [0.91-1.25]	0.87 [0.76-1.05]	0.008
LKCR ₂₀	1.14 [0.90-1.13]	1.19 [0.96-1.33]	0.89 [0.80-0.96]	0.009	1.20 [0.96-1.38]	0.91 [0.81-1.22]	0.012
CEI ₁₀	1.39 [1.27-1.57]	1.43 [1.34-1.58]	1.26 [1.22-1.32]	0.006	1.47 [1.34-1.58]	1.33 [1.25-1.38]	0.003
CEI ₂₀	1.43 [1.30-1.61]	1.45 [1.35-1.63]	1.32 [1.19-1.37]	0.007	1.50 [1.39-1.66]	1.35 [1.19-1.42]	0.001
HUI ₁₀	407.3 [223.7-640.9]	486.2 [235.3-845.4]	312.4 [-3.31-400]	0.022	522.4 [284.9-1036.4]	265.7 [130.5-383.7]	<0.001
HUI ₂₀	660.5 [301.5-956.5]	697.8 [367.1-1028.9]	265 [72.5-620.4]	0.009	720.1 [450.5-1062.4]	327.2 [198.1-772.2]	0.004

CEI10 and CEI20 = contrast enhancement index at 10-20 min; HUI = hepatic uptake index; LKCR10 and LKCR20 = liver-kidney contrast ratio at 10-20 min; LMCR10 and LMCR20 = liver-muscle contrast ratio at 10-20 min; LSCR10 and LSCR20 = liver-spleen contrast ratio at 10-20 min; N = number; NS = non-significant; RLE10 and RLE20 = relative liver enhancement at 10-20

quate HBP at 20 minutes were CP-B patients and all of them had CSPH. Contrarily, in all 19 patients without CSPH, the HBP was classified as adequate. Table 5 describes the different quantitative parameters evaluating the Gd-EOB-DTPA liver uptake in the 20 minutes HBP considering the quality of the HBP according to the subjective assessment. All indices were significantly higher in those studies classified as having an adequate HBP compared to those categorized as non-adequate. We further evaluated the impact of the quality of the HBP in the registration of the signal intensity of HCC lesions related to the surrounding liver parenchyma. At the 20 minutes HBP, 26 out of 41 HCC nodules (63.4%) were hypointense, 8 (19.5%) isointense, 6 hyperintense (14.6%) and 1 HCC (2.4%) was heterogenous. In the 49 patients with an adequate Gd-EOB-DTPA liver uptake, 25 out of 32 HCC nodules (78.1%) were hypointense. Contrarily, in the 12 patients with non-adequate Gd-EOB-DTPA liver uptake, one of the 9 nodules diagnosed as HCC were hypointense ($p < 0.001$). We further compared the appearance of HCC in the HBP according to the presence of CSPH. In the 19 patients without CSPH, 12 out of 14 HCCs (85.7%) were hypointense. On the other hand, only 14 out of 27 HCCs (51.9%) in the 43 patients with CSPH appeared as hypointense ($p = 0.044$).

Discussion

The results of our study show that the presence of CSPH in cirrhotic patients determines an impairment of the liver Gd-EOB-DTPA uptake reflected by significant lower values by almost all quantitative indices evaluated. In addition, the patients with healthy liver displayed more intense liver contrast uptake during the 10 minutes HBP, even when they were compared with cirrhotic patients with very well-preserved liver function defined as Child-Pugh A 5 points and absence of CSPH. Very interestingly, the rate of hypointense HCC in the HBP is significantly lower in those patients with CSPH, having an impact on HCC detection by MR with Gd-EOB-DTPA. Our findings are clinically relevant since cirrhotic patients who present CSPH and impaired liver function are those at high risk of HCC development in whom an early diagnosis and accurate tumor staging are critical. This fact represents a severe limitation for the detection of new HCC nodules in cirrhotic patients when dynamic sequences are skipped in the abbreviated MRI protocol for the HCC screening.²⁸⁻³¹

There are several hypotheses that could justify the suboptimal HBP in the cirrhotic liver. The potential decrease in the number of hepatocytes due to the increase of fibrous tissue in the cirrhotic

TABLE 3. Quantitative assessment of liver uptake of Gadolinium-ethoxybenzyl-diethylenetriamine penta-acetic acid (Gd-EOB-DTPA) during hepatobiliary phase (HPB) at 10 and 20 minutes in the study group considering the presence of clinically significant portal hypertension (CSPH). On the left, including all study cohort and on the right, considering only cirrhotic patients with preserved liver function (Child-Pugh A 5 points). Variables described as median and interquartile range

INDEX	All study cohort			Cirrhotic patients with preserved liver function (Child-Pugh A 5 points)		
	No CSPH (all CP A-5 points)	CSPH	P value	No CSPH (all CP A-5 points)	CP A-5 points and CSPH	P value
N	19	43		19	25	
RLE₁₀	0.73 [0.52-0.89]	0.57 [0.47-0.69]	0.027	0.73 [0.52-0.89]	0.65 [0.51-0.77]	NS
RLE₂₀	0.73 [0.56-0.85]	0.59 [0.47-0.74]	NS	0.73 [0.56-0.85]	0.66 [0.54-0.77]	NS
LSCR₁₀	1.54 [1.37-1.67]	1.23 [1.15-1.39]	< 0.001	1.54 [1.37-1.67]	1.29 [1.15-1.51]	0.014
LSCR₂₀	1.68 [1.53-1.84]	1.35 [1.20-1.57]	0.003	1.68 [1.53-1.84]	1.37 [1.26-1.74]	0.036
LMCR₁₀	2.41 [2.12-2.83]	2.06 [1.75-2.45]	0.006	2.41 [2.12-2.83]	1.88 [1.76-2.50]	0.034
LMCR₂₀	2.49 [2.24-2.96]	1.95 [1.77-2.39]	0.005	2.49 [2.24-2.96]	1.92 [1.78-2.6]	0.036
LKCR₁₀	1.15 [0.98-1.34]	0.93 [0.81-1.13]	0.001	1.15 [0.98-1.34]	1.01 [0.84-1.21]	0.032
LKCR₂₀	1.25 [1.16-1.43]	0.98 [0.88-1.28]	0.001	1.25 [1.16-1.43]	1.05 [0.88-1.03]	0.017
CEI₁₀	1.46 [1.34-1.59]	1.36 [1.26-1.52]	NS	1.46 [1.34-1.59]	1.47 [1.31-1.58]	NS
CEI₂₀	1.50 [1.38-1.71]	1.41 [1.24-1.54]	NS	1.50 [1.38-1.71]	1.48 [1.33-1.65]	NS
HUI₁₀	609.7 [501.4-970.3]	327.8 [191.7-511.8]	0.004	609.7 [501.4-970.3]	411.4 [223.4-1210.7]	NS
HUI₂₀	803.6 [678.7-1091.2]	450.5 [274.8-864.4]	0.033	803.6 [678.7-1091.2]	569.0 [341.8-987.1]	NS

CEI10 and CEI20 = contrast enhancement index at 10-20 min; HUI = hepatic uptake index; LKCR10 and LKCR20 = liver-kidney contrast ratio at 10-20 min; LMCR10 and LMCR20 = liver-muscle contrast ratio at 10-20 min; LSCR10 and LSCR20 = liver-spleen contrast ratio at 10-20 min; N = number; NS = non-significant; RLE10 and RLE20 = relative liver enhancement at 10-20 min

TABLE 4. Quantitative assessment of liver uptake of Gadolinium-ethoxybenzyl-diethylenetriamine penta-acetic acid (Gd-EOB-DTPA) during hepatobiliary phase (HPB) at 10 minutes in patients with normal liver (control group) compared with all Child-Pugh (CP) A 5 points patients (left panel) and with patients Child-Pugh A 5 points patients without clinically significant portal hypertension (CSPH). Variables described as median and interquartile range

INDEX	All Child-Pugh A 5 points patients		Child-Pugh A 5 points patients without clinically significant portal hypertension (CSPH)			
	Control group	Child-Pugh A-5 points	Control group	No CSPH (all CP A-5 points)		
N	20	44	20	19		
RLE₁₀	1.06 [0.82-2.16]	0.68 [0.52-0.82]	< 0.001	1.06 [0.82-2.16]	0.73 [0.52-0.89]	< 0.001
LSCR₁₀	2.27 [2.06-2.88]	1.43 [1.19-1.61]	< 0.001	2.27 [2.06-2.88]	1.54 [1.37-1.67]	< 0.001
LMCR₁₀	3.11 [2.90-3.55]	2.26 [1.81-2.71]	< 0.001	3.11 [2.90-3.55]	2.41 [2.12-2.83]	< 0.001
LKCR₁₀	1.82 [1.51-1.99]	1.06 [0.91-1.25]	< 0.001	1.82 [1.51-1.99]	1.15 [0.98-1.34]	< 0.001
CEI₁₀	1.71 [1.55-1.85]	1.47 [1.34-1.58]	0.001	1.71 [1.55-1.85]	1.46 [1.34-1.59]	0.007
HUI₁₀	1449.6 [1259-1717.7]	522.4 [284.9-1036.4]	< 0.001	1449.6 [1259-1717.7]	609.7 [501.4-970.3]	< 0.001

CEI10 = contrast enhancement index at 10 min; HUI = hepatic uptake index; LKCR10 = liver-kidney contrast ratio at 10 min; LMCR10 = liver-muscle contrast ratio at 10 min; LSCR10 = liver-spleen contrast ratio at 10 min; N = number; RLE10 = relative liver enhancement at 10 min

liver may have a role^{10,32} and also, the eventual alteration of the Gd-EOB-DTPA transport system in the hepatocellular membrane, with decrease of the expression of the organic anion transporting polypeptides (OATP1B1 and OATP1B3) and/or the increase of the multidrug resistance protein MRP2 expression.^{6,32,33} Furthermore, structural and biochemical changes at the sinusoidal system may also contribute to a suboptimal HBP in the MR

with Gd-EOB-DTPA, as shown in the sinusoidal obstruction syndrome (SOS), characterized by sinusoidal congestion and dilatation due to detachment of the cellular endothelium that obstructs the sinusoidal fenestrations in the centrilobular space, associated with hepatocellular necrosis and perisinusoidal fibrosis.^{34,35}

To our knowledge, there are few studies evaluating the impact of PH in the Gd-EOB-DTPA MR.

TABLE 5. Quantitative parameters evaluating the liver uptake in the 20 minutes hepatobiliary phase (HPB) of Gadolinium-ethoxybenzyl-diethylenetriamine penta-acetic acid (Gd-EOB-DTPA) according to the quality of the HBP. In one patient the HBP at 20 minutes was not available (n = 61). Variables described as median and interquartile range

INDEX	Qualitative assessment adequate	Qualitative assessment Non-adequate	P value
N	49	12	
RLE ₂₀	0.68 [0.57-0.83]	0.40 [0.31-0.51]	< 0.001
LSCR ₂₀	1.53 [1.34-1.78]	1.19 [1.06-1.22]	< 0.001
LMCR ₂₀	2.34 [1.88-2.78]	1.91 [1.50-2.11]	0.002
LKCR ₂₀	1.20 [0.95-1.35]	0.89 [0.78-0.98]	0.001
CEI ₂₀	1.23 [1.09-1.32]	1.00 [0.90-1.10]	0.001
HUI ₂₀	744.1 [444.8-1024.1]	251.5 [65-4-331.0]	< 0.001

CEI10 and CEI20 = contrast enhancement index at 10-20 min; HUI = hepatic uptake index; LKCR10 and LKCR20 = liver-kidney contrast ratio at 10-20 min; LMCR10 and LMCR20 = liver-muscle contrast ratio at 10-20 min; LSCR10 and LSCR20 = liver-spleen contrast ratio at 10-20 min; N = number; RLE10 and RLE20 = relative liver enhancement at 10-20 min

Asenbaum *et al.*³⁶ included in a retrospective study 178 patients with chronic liver disease without superimposed HCC, 109 (61.2%) with CSPH. The authors demonstrated an inverse correlation between HVPG and RLE ($r2 = 0.18$, $p < 0.0001$), findings in line with our results. Regrettably, in this study the authors did not include a control group and thus, were not able to demonstrate the worse contrast uptake in the HBP in cirrhotics without CSPH compared with healthy liver patients. In addition, in our study the quantitative analysis of the contrast uptake was done not only by the measurement of RLE, but also by the determination of contrast enhancement index, hepatic uptake index, and liver to spleen, muscle and kidney contrast indices, thus confirming the impact of CSPH in the Gd-EOB-DTPA hepatocyte uptake. More recently, Hectors *et al.* conducted a prospective study with 35 patients with chronic liver disease who underwent HVPG measurements and dynamic Gd-EOB-DTPA MR. Twenty-one (60%) patients had PH, of whom 9 had CSPH, and the authors report a statistically significant decrease of liver contrast uptake in presence of CSPH.³⁷

A very relevant finding of our study is the unexpected high rate of HCC nodules that were hyper or isointense (36.6%) compared to the surrounding liver parenchyma in the HBP, since previous studies have described that less than 15% of HCC nodules were not hypointense in the HBP.^{8,28,38-40} Interestingly, this rate is significantly higher in those patients with CSPH (48.1%) compared to those without (14.3%). This finding is supported

by the poorer contrast uptake of the non-tumoral liver parenchyma in those patients with CSPH. Consequently, the diagnostic capacity of Gd-EOB-DTPA is significantly impaired in those patients at higher risk of HCC and thus, in higher need of properly establishing if a hepatic nodule corresponds to a malignant focus or not. According to our results, portal pressure determines the target population for the optimal use of Gd-EOB-DTPA MR in patients with chronic liver disease, and those patients with no CSPH potentially candidates to resection in case an early HCC is diagnosed may benefit most from Gd-EOB-DTPA MR.

Our study has some limitations. First, it includes a small number of patients and the number of patients with no CSPH or with impaired liver function was relatively low. Finally, it could be argued that the determination of CSPH was done invasively in 11 out of 43 cases. However, we applied a very stringent, internationally validated non-invasive criteria based on available evidence, which minimizes a potential misclassification. Finally, we did not conduct T1 relaxation time measurements at HBP, which has been suggested as an accurate approach for evaluating liver function.^{41,42}

In conclusion, our study shows that the liver uptake of Gd-EOB-DTPA at the HBP is impaired in cirrhosis compared to healthy livers regardless the degree of liver function impairment. Even in patients with compensated cirrhosis categorized as CP-A 5 points, the liver contrast uptake is impaired when CSPH is present. This limits the ability to register hypointensity in the HBP and thus, hampers the detection capacity of HCC when using MR with organ-specific contrast and the dynamic sequences are skipped of the MRI protocol for HCC screening.

Acknowledgments

This is a post-hoc analysis from an investigator-initiated study partially funded by an unrestricted grant by Bayer Healthcare. CIBEREHD is funded by Instituto de Salud Carlos III. Dr. Alejandro Forner is partially supported by Instituto de Salud Carlos III (PI13/01229 and PI18/00542). Dr. Jordi Rimola is partially supported by grant from European Association for the Study of the Liver (EASL). Dr. María Reig is partially supported by Instituto de Salud Carlos III (PI15/00145 and PI18/0358) and from the Spanish Health Ministry (National Strategic Plan against Hepatitis C). Dr. Jordi Bruix is partially supported by Instituto de

Salud Carlos III (PI18/00768), the Spanish Health Ministry (National Strategic Plan against Hepatitis C) and AECC (PI044031).

References

- Bosch J, Groszmann RJ, Shah VH. Evolution in the understanding of the pathophysiological basis of portal hypertension: how changes in paradigm are leading to successful new treatments. *J Hepatol* 2015; **62**: S121-30. doi: 10.1016/j.jhep.2015.01.003
- de Franchis R, Baveno VI Faculty. Expanding consensus in portal hypertension. *J Hepatol* 2015; **63**: 743-52. doi: 10.1016/j.jhep.2015.05.022
- Ripoll C, Groszmann RJ, Garcia-Tsao G, Bosch J, Grace N, Burroughs A, et al. Hepatic venous pressure gradient predicts development of hepatocellular carcinoma independently of severity of cirrhosis. *J Hepatol* 2009; **50**: 923-8. doi: 10.1016/j.jhep.2009.01.014
- Reig M, Forner A, Rimola J, Ferrer-Fàbrega J, Burrel M, García-Criado A, et al. BCLC strategy for prognosis prediction and treatment recommendation Barcelona Clinic Liver Cancer (BCLC) staging system. The 2022 update. *J Hepatol* 2022; **76**: 681-93. doi: 10.1016/j.jhep.2021.11.018
- Galle PR, Forner A, Llovet JM, Mazzaferro V, Piscaglia F, Raoul JL, et al. EASL Clinical Practice Guidelines: management of hepatocellular carcinoma. *J Hepatol* 2018; **69**: 182-236. doi: 10.1016/j.jhep.2018.03.019
- Van Beers BE, Pastor CM, Hussain HK. Primovist, Eovist: what to expect? *J Hepatol* 2012; **57**: 421-9. doi: 10.1016/j.jhep.2012.01.031
- Kitao A, Zen Y, Matsui O, Gabata T, Kobayashi S, Koda W, et al. Hepatocellular carcinoma: signal intensity at gadoxetic acid-enhanced MR Imaging – correlation with molecular transporters and histopathologic features. *Radiology* 2010; **256**: 817-26. doi: 10.1148/radiol.10092214
- Choi JW, Lee JM, Kim SJ, Yoon JH, Baek JH, Han JK, et al. Hepatocellular carcinoma: imaging patterns on gadoxetic acid-enhanced MR Images and their value as an imaging biomarker. *Radiology* 2013; **267**: 776-86. doi: 10.1148/radiol.13120775
- Ricke J, Seidensticker M. Molecular imaging and liver function assessment by hepatobiliary MRI. *J Hepatol* 2016; **65**: 1081-2. doi: 10.1016/j.jhep.2016.10.004
- Kukuk GM, Schaefer SG, Fimmers R, Hadizadeh DR, Ezziddin S, Spengler U, et al. Hepatobiliary magnetic resonance imaging in patients with liver disease: correlation of liver enhancement with biochemical liver function tests. *Eur Radiol* 2014; **24**: 2482-90. doi: 10.1007/s00330-014-3291-x
- Kobi M, Paroder V, Flusberg M, Rozenblit AMM, Chernyak V. Limitations of Gd-EOB-DTPA-enhanced MRI: can clinical parameters predict suboptimal hepatobiliary phase? *Clin Radiol* 2017; **72**: 55-62. doi: 10.1016/j.crad.2016.10.004
- Okada M, Murakami T, Kuwatsuru R, Nakamura Y, Isoda H, Goshima S, et al. Biochemical and clinical predictive approach and time point analysis of hepatobiliary phase liver enhancement on Gd-EOB-DTPA-enhanced MR images: a multicenter study. *Radiology* 2016; **281**: 474-83. doi: 10.1148/radiol.2016151061
- Zhang W, Wang X, Miao Y, Hu C, Zhao W. Liver function correlates with liver-to-portal vein contrast ratio during the hepatobiliary phase with Gd-EOB-DTPA-enhanced MR at 3 Tesla. *Abdom Radiol* 2018; **43**: 2262-9. doi: 10.1007/s00261-018-1462-y
- Öcal O, Peynircioglu B, Loewe C, van Delden O, Vandecaveye V, Gebauer B, et al. Correlation of liver enhancement in gadoxetic acid-enhanced MRI with liver functions: a multicenter-multivendor analysis of hepatocellular carcinoma patients from SORAMIC trial. *Eur Radiol* 2021; **32**: 1320-9. doi: 10.1007/s00330-021-08218-9
- Liang M, Zhao J, Xie B, Li C, Yin X, Cheng L, et al. MR liver imaging with Gd-EOB-DTPA: The need for different delay times of the hepatobiliary phase in patients with different liver function. *Eur J Radiol* 2016; **85**: 546-52. doi: 10.1016/j.ejrad.2015.12.015
- Ippolito D, Famularo S, Giani A, Orsini EB, Pecorelli A, Pinotti E, et al. Estimating liver function in a large cirrhotic cohort: Signal intensity of gadolinium-ethoxybenzyl-diethylenetriamine penta-acetic acid-enhanced MRI. *Dig Liver Dis* 2019; **51**: 1438-45. doi: 10.1016/j.dld.2019.04.009
- Yoon JH, Choi JJ, Jeong YY, Schenk A, Chen L, Laue H, et al. Pre-treatment estimation of future remnant liver function using gadoxetic acid MRI in patients with HCC. *J Hepatol* 2016; **65**: 1155-62. doi: 10.1016/j.jhep.2016.07.024
- Yoon JH, Lee JM, Kang H, Ahn SJ, Yang H, Kim E, et al. Quantitative assessment of liver function by using Gadoxetic Acid-enhanced MRI: hepatocyte uptake ratio. *Radiology* 2019; **290**: 125-33. doi: 10.1148/radiol.2018180753
- Yamada S, Shimada M, Morine Y, Imura S, Ikemoto T, Saito Y, et al. A new formula to calculate the resection limit in hepatectomy based on Gd-EOB-DTPA-enhanced magnetic resonance imaging. *PLoS One* 2019; **14**: e0210579. doi: 10.1371/journal.pone.0210579
- Notake T, Shimizu A, Kubota K, Ikehara T, Hayashi H, Yasukawa K, et al. Hepatocellular uptake index obtained with gadoxetate disodium-enhanced magnetic resonance imaging in the assessment future liver remnant function after major hepatectomy for biliary malignancy. *BJS Open* 2021; **55(4)**: zraa048. doi: 10.1093/BJSOPEN/ZRAA048
- Daire JL, Leporq B, Vilgrain V, Van Beers BE, Schmidt S, Pastor CM. Liver perfusion modifies Gd-DTPA and Gd-BOPTA hepatocyte concentrations through transfer clearances across sinusoidal membranes. *Eur J Drug Metab Pharmacokin* 2017; **42**: 657-67. doi: 10.1007/s13318-016-0382-x
- Ayuso C, Forner A, Darnell A, Rimola J, García-Criado Á, Bianchi L, et al. Prospective evaluation of gadoxetic-acid MR for the diagnosis of HCC in newly detected nodules ≤ 2 cm in cirrhosis. *Liver Int* 2019; **39**: 1281-91. doi: 10.1111/liv.14133
- Llop E, Berzigotti A, Reig M, Erice E, Reverter E, Seijo S, et al. Assessment of portal hypertension by transient elastography in patients with compensated cirrhosis and potentially resectable liver tumors. *J Hepatol* 2012; **56**: 103-8. doi: 10.1016/j.jhep.2011.06.027
- Neri E, Bali MA, Ba-Ssalamah A, Boraschi P, Brancatelli G, Alves FC, et al. ESGAR consensus statement on liver MR imaging and clinical use of liver-specific contrast agents. *Eur Radiol* 2016; **26**: 921-31. doi: 10.1007/s00330-015-3900-3
- Ba-Ssalamah A, Bastati N, Wibmer A, Fragner R, Hodge JC, Trauner M, et al. Hepatic gadoxetic acid uptake as a measure of diffuse liver disease: where are we? *J Magn Reson Imaging* 2017; **45**: 646-59. doi: 10.1002/jmri.25518
- Motosugi U, Ichikawa T, Oguri M, Sano K, Sou H, Muhi A, et al. Staging liver fibrosis by using liver-enhancement ratio of gadoxetic acid-enhanced MR imaging: comparison with aspartate aminotransferase-to-platelet ratio index. *Magn Reson Imaging* 2011; **29**: 1047-52. doi: 10.1016/j.mri.2011.05.007
- Watanabe H, Kanematsu M, Goshima S, Kondo H, Onozuka M, Moriyama N, et al. Staging hepatic fibrosis: comparison of Gadoxetate Disodium-enhanced and diffusion-weighted MR imaging – preliminary observations. *Radiology* 2011; **259**: 142-50. doi: 10.1148/radiol.10100621
- Besa C, Lewis S, Pandharipande PV, Chhatwal J, Kamath A, Cooper N, et al. Hepatocellular carcinoma detection: diagnostic performance of a simulated abbreviated MRI protocol combining diffusion-weighted and T1-weighted imaging at the delayed phase post gadoxetic acid. *Abdom Radiol* 2017; **42**: 179-90. doi: 10.1007/s00261-016-0841-5
- Vietti Violi N, Taouli B. Abbreviated MRI for HCC surveillance: is it ready for clinical use? *Eur Radiol* 2020; **30**: 4147-9. doi: 10.1007/s00330-020-06904-8
- Canellas R, Rosenkrantz AB, Taouli B, Sala E, Saini S, Pedrosa I, et al. Abbreviated MRI protocols for the abdomen. *Radiographics* 2019; **39**: 744-58. doi: 10.1148/rg.2019180123
- Koh DM, Ba-Ssalamah A, Brancatelli G, Fananapazir G, Fiel MI, Goshima S, et al. Consensus report from the 9th International Forum for Liver Magnetic Resonance Imaging: applications of gadoxetic acid-enhanced imaging. *Eur Radiol* 2021; **31**: 5615-28. doi: 10.1007/S00330-020-07637-4
- Hanada K, Nakai K, Tanaka H, Suzuki F, Kumada H, Ohno Y, et al. Effect of nuclear receptor downregulation on hepatic expression of cytochrome P450 and transporters in chronic hepatitis C in association with fibrosis development. *Drug Metab Pharmacokin* 2012; **27**: 301-6. doi: 10.2133/dmpk.dmpk-11-rg-077
- Thakkar N, Slizgi JR, Brouwer KLR. Effect of liver disease on hepatic transporter expression and function. *J Pharm Sci* 2017; **106**: 2282-94. doi: 10.1016/j.xphs.2017.04.053
- Shin NY, Kim MJ, Lim JS, Park MS, Chung YE, Choi JY, et al. Accuracy of gadoxetic acid-enhanced magnetic resonance imaging for the diagnosis of sinusoidal obstruction syndrome in patients with chemotherapy-treated colorectal liver metastases. *Eur Radiol* 2012; **22**: 864-71. doi: 10.1007/s00330-011-2333-x

35. Yoneda N, Matsui O, Ikeno H, Inoue D, Yoshida K, Kitao A, et al. Correlation between Gd-EOB-DTPA-enhanced MR imaging findings and OATP1B3 expression in chemotherapy-associated sinusoidal obstruction syndrome. *Abdom Imaging* 2015; **40**: 3099-103. doi: 10.1007/s00261-015-0503-z
36. Asenbaum U, Ba-Ssalamah A, Mandorfer M, Nolz R, Furtner J, Reiberger T, et al. Effects of portal hypertension on Gadoxetic Acid-Enhanced liver magnetic resonance: diagnostic and prognostic implications. *Invest Radiol* 2017; **52**: 462-9. doi: 10.1097/RLI.0000000000000366
37. Hectors SJ, Bane O, Kennedy P, Cuevas J, Thung S, Fischman A, et al. Noninvasive diagnosis of portal hypertension using gadoxetate DCE-MRI of the liver and spleen. *Eur Radiol* 2021; **31**: 4804-12. doi: 10.1007/s00330-020-07495-0
38. Choi JY, Lee JM, Sirlin CB. CT and MR imaging diagnosis and staging of hepatocellular carcinoma. Part II. Extracellular agents, hepatobiliary agents, and ancillary imaging features. *Radiology* 2014; **273**: 30-50. doi: 1148/radiol.14132362
39. Renzulli M, Golfieri R, Bologna Liver Oncology Group (BLOG). Proposal of a new diagnostic algorithm for hepatocellular carcinoma based on the Japanese guidelines but adapted to the Western world for patients under surveillance for chronic liver disease. *J Gastroenterol Hepatol* 2016; **31**: 69-80. doi: 10.1111/jgh.13150
40. Renzulli M, Biselli M, Brocchi S, Granito A, Vasuri F, Tovoli F, et al. New hallmark of hepatocellular carcinoma, early hepatocellular carcinoma and high-grade dysplastic nodules on Gd-EOB-DTPA MRI in patients with cirrhosis: a new diagnostic algorithm. *Gut* 2018; **67**: 1674-82. doi: 10.1136/gutjnl-2017-315384
41. Ding Y, Rao SX, Chen C, Li R, Zeng MS. Assessing liver function in patients with HBV-related HCC: a comparison of T1 mapping on Gd-EOB-DTPA-enhanced MR imaging with DWI. *Eur Radiol* 2015; **25**: 1392-8. doi: 10.1007/s00330-014-3542-x
42. Haimerl M, Verloh N, Zeman F, Fellner C, Müller-Wille R, Schreyer AG, et al. Assessment of clinical signs of liver cirrhosis using T1 mapping on Gd-EOB-DTPA-enhanced 3T MRI. *PLoS One* 2013; **8**: e85658 doi: 10.1371/JOURNAL.PONE.0085658